

# Solid-State NMR Spectroscopy Reveals that *E. coli* Inclusion Bodies of HET-s(218–289) are Amyloids\*\*

Christian Wasmer, Laura Benkemoun, Raimon Sabaté, Michel O. Steinmetz, Bénédicte Coulary-Salin, Lei Wang, Roland Riek, Sven J. Saupe, and Beat H. Meier\*

Heterologous protein expression in *E. coli* has taken on tremendous importance in many fields of biology since it allows the preparation of sufficient amounts of sample for physicochemical investigations.<sup>[1]</sup> Often, however, expressed proteins are deposited as insoluble aggregates, the so-called inclusion bodies (IBs).<sup>[2]</sup> The formation of IBs—dense intracellular deposits of amorphous appearance that can reach 1  $\mu\text{m}^3$  in volume<sup>[3]</sup>—is often regarded as an obstacle that prevents the isolation of native heterologous proteins from *E. coli* cells. However, the formation of IBs can also be beneficial in some applications, as it allows the recovery of large amounts of pure protein. In the context of structural biology, the deposition of aggregated protein in IBs is of interest because it may be closely related to the formation of amyloid deposits associated with many diseases.<sup>[4]</sup> However, while IBs were often regarded as unspecific aggregates, fibrils were, in contrast, thought to be ordered. The postulate now emerges that IB formation and fibrilization are both nucleation-driven processes governed by sequence-specific protein interactions which lead to the formation of specific  $\beta$ -sheet-rich aggregates. Recent structural studies that used quenched H/D exchange (by NMR spectroscopy), fiber diffraction, microscopy, IR spectroscopy, and mutagenesis have led to the postulation that inclusion bodies are closely related to amyloids.<sup>[5–7]</sup> However, a high-resolution structural comparison of a protein in both states has not been available until now.

In prions, protein aggregation becomes self-perpetuating in vivo, and is considered as a fundamental process for infectivity. [Het-s] is a prion of the filamentous fungus *Podospora anserina* involved in a fungal self-/non-self-recog-

nition phenomenon.<sup>[8]</sup> Previous studies have identified the C-terminal region spanning residues 218 to 289 of HET-s as the prion-forming domain.<sup>[9,10]</sup> In its infectious amyloid form, HET-s(218–289) forms a  $\beta$ -solenoid with two layers of  $\beta$  strands per monomer and is characterized by the formation of a triangular hydrophobic core.<sup>[11]</sup> [Het-s] prion infectivity can be observed in fibrils assembled in vitro<sup>[12,13]</sup> and seems to be associated with the structurally characterized amyloid fibrils obtained at pH 7. Alternative aggregated forms of HET-s, including amyloid forms obtained at low pH values, lack [Het-s] prion infectivity<sup>[13,14]</sup> in the sense of Ref. [15].

Herein we describe a structural and functional characterization of HET-s(218–289) IBs produced in *E. coli* by using electron microscopy (EM), NMR spectroscopy to determine H/D exchange, solid-state NMR spectroscopy, and in vivo prion infectivity assays as described earlier.<sup>[16]</sup>

HET-s(218–289) was expressed in *E. coli* cells and located as typical angular-shaped inclusions with high electron density and a cross-section of 100–400 nm preferentially at the cellular poles (Figure 1 and Figure S1 in the Supporting

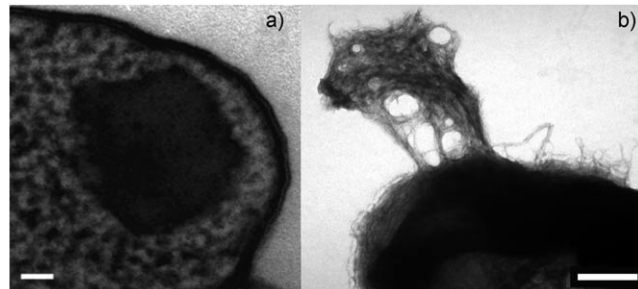


**Figure 1.** a) HET-s(218–289) IBs from *E. coli* observed by cryo-electron microscopy of entire *E. coli* cells. b) Transmission electron micrograph of negatively stained purified HET-s(218–289) IBs. Scale bars: a) 50 nm and b) 200 nm.

Information). The IBs were partially purified (see the Supporting Information) and this material was shown by EM (Figure 1b) to consist of fibrillar structures. The purified material was then used to infect prion-free *P. anserina* strains by using a protein transfection method as previously described.<sup>[16]</sup> While insoluble extracts from an *E. coli* control strain containing only the empty vector or IBs of a different protein (human NDP kinase) did not induce the appearance of the prion form [Het-s] (Table 1), strains transfected with HET-s(218–289) IBs acquired [Het-s] at a frequency comparable to or even higher than that found for transfection with HET-s(218–289) amyloids assembled in vitro. We conclude

[\*] C. Wasmer, Dr. L. Wang, Prof. R. Riek, Prof. B. H. Meier  
Laboratorium für Physikalische Chemie, ETH Zurich  
8093 Zurich (Switzerland)  
Fax: (+41) 446-321-621  
E-mail: beme@ethz.ch

Dr. L. Benkemoun, Dr. R. Sabaté, Dr. B. Coulary-Salin, Dr. S. J. Saupe  
Laboratoire de Génétique Moléculaire des Champignons  
IBGC UMR 5095 CNRS, Université de Bordeaux 2  
Bordeaux (France)  
Dr. M. O. Steinmetz  
Biomolecular Research, Structural Biology  
Paul Scherrer Institut  
5232 Villigen (Switzerland)

[\*\*] We thank Dr. J. Greenwald, Dr. H. Van Melckebeke, Dr. A. Lange, and Dr. M. Ernst for helpful discussions. This research was supported by the Swiss National Science Foundation.

Supporting information for this article is available on the WWW under <http://dx.doi.org/10.1002/anie.200806100>.

**Table 1:** Prion infectivity assays with *E. coli* HET-s(218–289) IBs.<sup>[a]</sup>

Protein	Amount of protein in transfection reaction [pmol]					
	2000	1000	500	200	100	50
insoluble <i>E. coli</i> extract of <i>E. coli</i> strain with empty vector	3/138 <sup>[b]</sup>					
NDP kinase IBs	n.d.	n.d.	5/84	n.d.	n.d.	n.d.
HET-s(218–289) fibrils	n.d.	17/24	44/60	31/72	7/24	5/24
HET-s(218–289) IBs	n.d.	23/24	58/60	34/72	15/24	13/24
HET-s(218–289) IBs (purified NMR sample)	24/24	nd	45/48	n.d.	n.d.	n.d.

[a] In each case, the number of prion-infected strains over the total number of tested strains is given; n.d.: not determined. [b] The amount of insoluble *E. coli* extract used corresponds to the amount of cells that yield about 0.5 nmol of HET-s(218–289) IBs.

from these experiments that HET-s(218–289) IBs display [HET-s] prion infectivity, thus indicating that HET-s(218–289) acquires an infectious prion fold in *E. coli* IBs.

Next, a set of experiments was performed in which further properties of the HET-s IBs and amyloid fibrils assembled in vitro were compared. We found, in particular, that full-length HET-s or HET-s(157–289) inclusion bodies display the same 8 kDa proteinase K resistant core as HET-s and HET-s(157–289) amyloid fibrils assembled in vitro.<sup>[9,17]</sup> Moreover, both types of HET-s(218–289) aggregates (IBs and fibrils) display similar chemical denaturation properties: In particular, both are resistant to urea denaturation at neutral pH, but highly sensitive to urea denaturation at pH 2 (see Figure S2B in the Supporting Information). Finally, we found that HET-s(218–289) IBs, similar to HET-s(218–289) prion amyloids, could act as seeds for the formation of HET-s(218–289) amyloid in vitro (see Figure S3 in the Supporting Information).<sup>[13]</sup> It is also of note here that mutations in the 218–289 region that prevent the formation of the amyloid prion fold<sup>[10,18]</sup> also prevent the formation of IBs in *E. coli* (see Table S1 in the Supporting Information). Collectively, these results further emphasize the similarities between HET-s(218–289) IBs and HET-s(218–289) amyloid fibrils.

To characterize the HET-s(218–289) IBs on a molecular level we recorded solid-state NMR spectra and compared them with previously assigned spectra of the prion fibrils assembled in vitro,<sup>[19]</sup> whose structure was known.<sup>[11]</sup> The so-called raw IBs, obtained by washing the insoluble fraction of the lysed cells in pure water, give rise to the <sup>13</sup>C-<sup>13</sup>C proton-driven spin-diffusion (PDS)<sup>[20,21]</sup> spectrum shown in Figure 2 (blue contours). The spectrum reproduces all the peaks visible for HET-s(218–289) fibrils assembled in vitro (red contours). The separate spectra of the two samples are given in Figure S5 in the Supporting Information. Additional resonances, not belonging to HET-s(218–289), appear in several regions of the spectrum and are tentatively assigned to phospholipids from the *E. coli* membrane (at around 34 ppm (the CH<sub>2</sub> groups of the hydrophobic tails) and between 60 and 100 ppm) as well as to other proteins and possibly RNA. The many carbonyl resonances with chemical shifts in the range of 180 ppm to 176 ppm (where only a few HET-s(218–289) resonances are present) indicate the abundance of proteins,

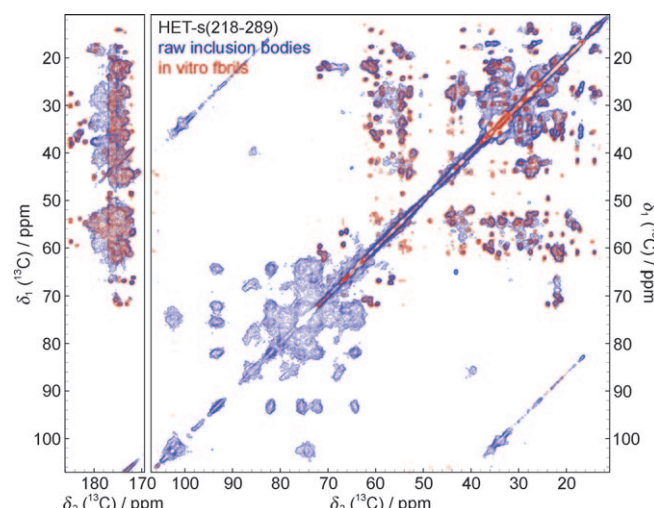


**Figure 2.** <sup>13</sup>C-<sup>13</sup>C solid-state NMR correlation spectrum (PDS) with a mixing time of 50 ms) of raw HET-s(218–289) IBs (blue) compared to a spectrum of purified and in vitro fibrillized HET-s(218–289) (red) recorded under identical conditions. All signals assigned for the purified fibrils were also observed in the spectrum of the IBs. The individual spectra were recorded at a <sup>1</sup>H frequency of 600 MHz (static field  $B_0 = 14.9$  T), 10 kHz MAS (MAS: magic angle spinning), and at about 3 °C, and are shown in Figure S4 in the Supporting Information.

most probably membrane proteins, with mainly  $\alpha$ -helical secondary structure.<sup>[22]</sup> The peaks assigned to HET-s(218–289) are already visible after a short expression time of 1 h (see Figure S7 in the Supporting Information). After further purification of the sample (see the Supporting Information), all the HET-s(218–289) resonances in the PDS spectrum are preserved, while the additional components are considerably reduced (Figure 3). The  $\alpha$ -helical proteins seem to be almost completely removed by the further purification procedure (see the carbonyl region). Considering the strong dependence of the NMR chemical shift on the conformation of a polypeptide chain, the identical chemical shifts of HET-s(218–289) in IBs and fibrils formed in vitro show that their molecular structures have to be virtually identical. Noticeably, the NMR linewidth of the resonances of the two samples is also indistinguishable, as judged from isolated signals in the 2D spectra (Figure 3, and Figure S6 in the Supporting Information), thus indicating a highly defined local molecular structure.<sup>[19]</sup> No indications of molecular polymorphism were found. The purified IB sample prepared for NMR studies was also found to display prion infectivity in transfection assays (Table 1).

In addition to the solid-state NMR spectroscopic characterization, an H/D exchange experiment was performed, as previously used for the characterization of the amyloid fibrils of HET-s(218–289).<sup>[10,23]</sup> The observed exchange pattern of the purified inclusion bodies closely resembles that of the in vitro fibrils of HET-s(218–289) (see Figure S8 in the Supporting Information), which further supports and verifies that the IBs and fibrils are virtually identical on a molecular level.

Our results indicate that the highly ordered amyloid HET-s(218–289) can be formed in the crowded milieu of the *E. coli* cell in the presence of folding modulators, chaperones, and

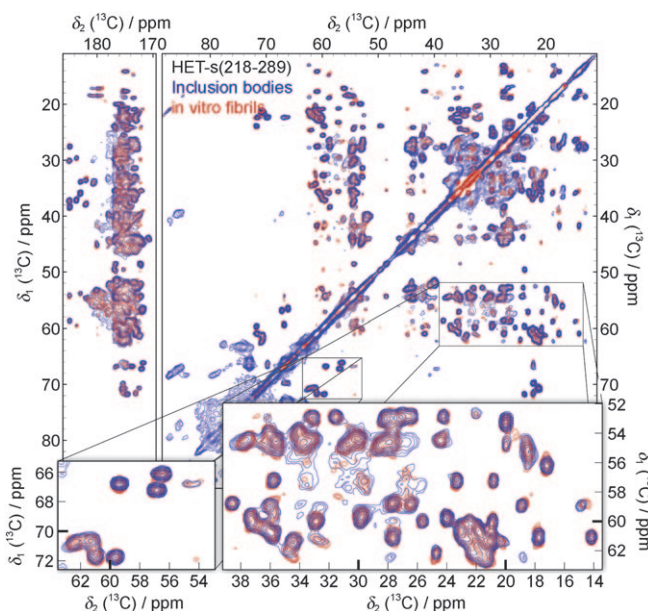


**Figure 3.**  $^{13}\text{C}$ - $^{13}\text{C}$  solid-state NMR correlation spectrum (PDSD with a mixing time of 50 ms) of purified HET-s(218-289) IBs (blue) compared to a spectrum of in vitro fibrillized HET-s(218-289) (red) recorded under identical conditions. All the signals assigned for the purified fibrils were also observed in the spectrum of the IBs. The insets demonstrate that no significant changes in the chemical shifts appear and that the linewidth of the two samples is virtually identical. The individual spectra were recorded at a  $^1\text{H}$  frequency of 600 MHz (static field  $B_0 = 14.9$  T), 10 kHz MAS, and at about 3 °C, and are shown in Figure S4 in the Supporting Information. One-dimensional slices are given in Figure S5 in the Supporting Information.

large amounts of other proteins. This observation is of particular importance in the context of the structural biology of prions, as it indicates that the fold characterized so far only in vitro can also form in a living cell. This also shows that inclusion bodies can be highly ordered in contrast to being “amorphous”, as could be inferred from their appearance in electron micrographs of in vivo material. The solid-state NMR spectra show that HET-s(218-289) adopts virtually the same molecular structure in IBs and in vitro fibrils, and thus show that the IBs consist in fact of amyloids. Careful inspection of the electron micrographs indeed gave clear evidence of fibrillar structures. Whether HET-s(218-289) represents an exception or whether other proteins can also display a highly ordered and functional amyloid structure in the bacterial inclusion body remains to be determined. For HET-s, in any case, it is clear that the formation of IBs and amyloid fibrils is a remarkably similar process and that the inclusion bodies are infectious and highly ordered at the molecular level. Evidence for amyloid-like behavior was

already found for IBs of the Alzheimer peptide  $\text{A}\beta(1-42)$ <sup>[6]</sup> and other proteins,<sup>[7]</sup> and our detailed atomic-level investigation of the HET-s system supports the emerging concept that amyloid formation is ubiquitous in living organisms and must be considered in the biotechnological production of protein.

Received: December 15, 2008

Revised: March 5, 2009

Published online: May 26, 2009

**Keywords:** amyloids · inclusion bodies · NMR spectroscopy · proteins · structure elucidation

- [1] F. Baneyx, *Curr. Opin. Biotechnol.* **1999**, *10*, 411.
- [2] F. Baneyx, M. Mujacic, *Nat. Biotechnol.* **2004**, *22*, 1399.
- [3] G. Georgiou, P. Valax, *Methods Enzymol.* **1999**, *309*, 48.
- [4] M. Carrió, N. González-Montalbán, A. Vera, A. Villaverde, S. Ventura, *J. Mol. Biol.* **2005**, *347*, 1025.
- [5] S. Ventura, A. Villaverde, *Trends Biotechnol.* **2006**, *24*, 179.
- [6] M. Morell, R. Bravo, A. Espargaro, X. Sisquella, F. Aviles, X. Fernandezbusquets, S. Ventura, *Biochim. Biophys. Acta Mol. Cell Res.* **2008**, *178*, 1815.
- [7] L. Wang, S. K. Maji, M. R. Sawaya, D. Eisenberg, R. Riek, *Plos Biol.* **2008**, *6*, e195.
- [8] V. Coustou, C. Deleu, S. J. Saupe, J. Begueret, *Proc. Natl. Acad. Sci. USA* **1997**, *94*, 9773.
- [9] A. Balguerie, S. Dos Reis, C. Ritter, S. Chaignepain, B. Coulary-Salin, V. Forge, K. Bathany, I. Lascu, J. Schmitter, R. Riek, S. J. Saupe, *EMBO J.* **2003**, *22*, 2071.
- [10] C. Ritter, M. L. Maddelein, A. B. Siemer, T. Luhrs, M. Ernst, B. H. Meier, S. J. Saupe, R. Riek, *Nature* **2005**, *435*, 844.
- [11] C. Wasmer, A. Lange, H. van Melckebeke, A. B. Siemer, R. Riek, B. H. Meier, *Science* **2008**, *319*, 1523.
- [12] M. L. Maddelein, *Med. Sci.* **2002**, *18*, 1187.
- [13] R. Sabaté, U. Baxa, L. Benkemoun, N. Sanchez de Groot, B. Coulary-Salin, M. Maddelein, L. Malato, S. Ventura, A. C. Steven, S. J. Saupe, *J. Mol. Biol.* **2007**, *370*, 768.
- [14] C. Wasmer, A. Soragni, R. Sabate, A. Lange, R. Riek, B. H. Meier, *Angew. Chem.* **2008**, *120*, 5923; *Angew. Chem. Int. Ed.* **2008**, *47*, 5839.
- [15] M. L. Maddelein, S. Dos Reis, S. Duvezin-Caubet, B. Coulary-Salin, S. J. Saupe, *Proc. Natl. Acad. Sci. USA* **2002**, *99*, 7402.
- [16] L. Benkemoun, R. Sabate, L. Malato, S. Dos Reis, H. Dalstra, S. J. Saupe, M. Maddelein, *Methods* **2006**, *39*, 61.
- [17] A. Balguerie, S. Dos Reis, B. Coulary-Salin, S. Chaignepain, M. Sabourin, J. M. Schmitter, S. J. Saupe, *J. Cell Sci.* **2004**, *117*, 2599.
- [18] M. Maddelein, *Prion* **2008**, *1*, 44.
- [19] A. B. Siemer, C. Ritter, M. Ernst, R. Riek, B. H. Meier, *Angew. Chem.* **2005**, *117*, 2494; *Angew. Chem. Int. Ed.* **2005**, *44*, 2441.
- [20] N. M. Szeverenyi, M. J. Sullivan, G. E. Maciel, *J. Magn. Reson.* **1982**, *47*, 462.
- [21] A. Grommek, B. H. Meier, M. Ernst, *Chem. Phys. Lett.* **2006**, *427*, 404.
- [22] Y. Wang, O. Jardetzky, *Protein Sci.* **2002**, *11*, 852.
- [23] M. Hoshino, H. Katou, Y. Hagiwara, K. Hasegawa, H. Naiki, Y. Goto, *Nat. Struct. Biol.* **2002**, *9*, 332.